Atmos. Chem. Phys. Discuss., 10, 19469–19514, 2010
www.atmos-chem-phys-discuss.net/10/19469/2010/
doi:10.5194/acpd-10-19469-2010

Atmospheric Chemistry and Physics Discussions

Tropical deep convection and its impact on composition in global and mesoscale models – Part 1: Meteorology and comparison with observations.

M. R. Russo[1], V. Marécal[2,5], C. R. Hoyle[3,4], J. Arteta[5], C. Chemel[6], M. P. Chipperfield[7], O. Dessens[8], W. Feng[7], J. S. Hosking[8,*], P. J. Telford[1], O. Wild[9], X. Yang[1], and J. A. Pyle[1]

[1]NCAS-Climate, Centre for Atmospheric Science, University of Cambridge, Cambridge, UK
[2]Laboratoire de Physique et Chimie de l'Environnement et de l'Espace, CNRS and University of Orléans, Orléans, France
[3]Department of Geosciences, University of Oslo, Norway
[4]Institute for Atmospheric and Climate Science, ETH Zurich, Zurich, Switzerland
[5]Centre National de Recherches Météorologique/Groupe d'étude de l'Atmosphère Météorologique, Météo-France and CNRS, Toulouse, France
[6]NCAS-Weather, Centre for Atmospheric & Instrumentation Research, University of Hertfordshire, Hatfield, UK

[7]Institute for Climate and Atmospheric Science, School of Earth and Environment, University of Leeds, UK
[8]Centre for Atmospheric Science, University of Cambridge, Cambridge, UK
[9]Lancaster Environment Centre, Lancaster University, UK
[*]now at: British Antarctic Survey, Cambridge, UK

Received: 19 July 2010 – Accepted: 11 August 2010 – Published: 19 August 2010

Correspondence to: M. R. Russo (maria.russo@atm.ch.cam.ac.uk)

Published by Copernicus Publications on behalf of the European Geosciences Union.

Abstract

Tropical convection is a very important atmospheric process acting on the water cycle, radiative budget of the atmosphere and air composition of the upper troposphere and lower stratosphere (UTLS), and it affects a broad range of spatial and temporal scales. The fast vertical transport in convective plumes can efficiently redistribute water vapour and pollutants up to the Tropical Tropopause Layer (TTL), and therefore affect the composition of the lower stratosphere. Chemistry Climate Models and Chemistry Transport Models are routinely used to study chemical processes in the atmosphere. In these models convection and convective transport of tracers are parameterised, and due to the interplay of chemical and dynamical processes, it has proven difficult to evaluate the convective transport of chemical species by comparison with observed chemical fields.

In this work we investigate different characteristics of tropical convection by using convective proxies from many independent observational datasets (including surface precipitation rates, cloud top pressure and OLR). We use observations to analyse the seasonal cycle and geographical preferences of convection, and its impact on water vapour. Using highly temporally resolved cloud top data we calculate the frequency distribution of high clouds in three tropical regions. The observational data is used as a benchmark for a number of numerical models, with a view to assess the ability of models to reproduce the seasonality, preferential location and vertical extent of tropical convection. Finally we discuss the implications of our findings on modelling the composition of the upper troposphere and lower stratosphere.

1 Introduction

Tropical deep convection is recognised as an important atmospheric feature acting on the global water cycle, radiative budget and chemical composition of the atmosphere. The vertical extent of convective plumes and their direct impact on stratospheric composition has been long debated (Danielsen, 1993; Smith et al., 2006;

Discussion Paper | Discussion Paper | Discussion Paper | Discussion Paper |

ACPD

10, 19469–19514, 2010

Modelling tropical convection: comparison with observations

M. R. Russo et al.

Ricaud et al., 2007; Levine et al., 2007; Berthet et al., 2007; Schiller et al., 2009). Convective events in the Tropics can routinely reach an altitude of 11–14 km, corresponding on average to 220–150 hPa (Gettelman et al., 2002; Alcala and Dessler, 2002) and occasionally can reach above the level of neutral buoyancy and penetrate directly above the tropopause at ∼16–17 km ("overshooting" convection, e.g. Highwood and Hoskins, 1998; Liu and Zipser, 2005; Grosvenor et al., 2007; Corti et al., 2008; Chemel et al., 2009). Although the frequency of convective events which directly penetrate into the lower stratosphere is thought to be very small (Liu and Zipser, 2005; Rossow and Pearl, 2007), deep convection can still play a role in determining the stratospheric composition through its interaction with the tropical tropopoause layer (TTL). The TTL is a transitional layer in the tropics connecting the upper troposphere (8–1 km) to the lower stratosphere (17 km) and it has been defined for example by Highwood and Hoskins, 1998; Folkins et al., 1999; Gettelman and Forster, 2002; Fueglistaler et al., 2009. This layer is of particular importance in troposphere-stratosphere exchanges, since it is from the TTL that chemical species and water vapour enter the lower stratosphere where they can influence the stratospheric composition on the global scale (Folkins et al., 1999; Sherwood and Dessler, 2001; Fueglistaler et al., 2004; Levine et al., 2007). Air from the boundary layer can be efficiently transported by deep convection into the TTL within a few hours (e.g. Pickering et al., 1996; Marécal et al., 2006). In the upper part of the TTL, i.e. above the level of zero net radiative heating ($Q = 0$ level), air parcels can be radiatively transported upward into the stratosphere, with a timescale of months (see Gettelmann et al., 2004 for estimates of heating rates). The height of the $Q = 0$ level has been estimated from radiative model calculations to be around 15 km for clear-sky conditions (Gettelman et al., 2004). Tropical convection can therefore affect stratospheric composition not only through direct injection of surface species into the stratosphere, but also through loading of the TTL region above the $Q = 0$ level. The frequency and location of convective events reaching above 15 km are therefore important elements in understanding the transport pathways of surface species and other pollutants to the lower stratosphere.

Because of its importance for both tropospheric and stratospheric air composition, tracer transport by tropical deep convection is taken into account in all types of 3-D atmospheric models dealing with tracers. Deep convection covers a large range of spatial scales from individual clouds with horizontal extent of a few square kilometres, to larger systems such as convective clusters of several thousands square kilometres. The horizontal resolution of current global models such as Chemistry Transport Models (CTMs), and General Circulation Models (GCMs) is typically 1–2 degrees or more in latitude/longitude. Numerical Weather Prediction (NWP) models have higher resolution with a grid spacing of ~0.5 degrees (equivalent to ~60 km) or smaller; they can be run globally or over a specific region, in which case they can also be referred to as Limited Area, regional or mesoscale models. However, even at these higher resolutions, most of the dynamical processes that lead to the onset and development of a convective plume occur on much smaller scales compared to the model grid, and as a result deep convection and the associated tracer transport cannot be explicitly represented. Therefore all these models make use of a parameterisation scheme to represent deep convection and the associated transport. Many such parameterisations have been proposed in the literature (e.g. Arakawa and Schubert, 1974; Tiedke, 1989; Kain and Fritch, 1990; Grell, 1993; Zhang and McFarlane, 1995). Previous studies showed that model simulations are strongly influenced by the convection parameterisation used (e.g. Mapes et al., 2004; Lawrence and Rasch, 2005; Yano, 2009; Arteta et al., 2009a; Tost et al., 2010). This is known to be a very significant source of uncertainties in global and regional models. The triggering and intensity of convection is also sensitive to model vertical and horizontal resolutions (e.g. Rind, 1988; Dequé et al., 1994; Pope et al., 2001; Arteta et al., 2009b). Because of these differences in horizontal and vertical resolution and in the treatment of advection and convection, models are likely to provide different locations, frequency and vertical extent of tropical convective events. This can lead to differences in the convective transport of tracers, possibly affecting air composition in the free troposphere and the TTL at the global scale. So far no attempt has been made to objectively compare and evaluate deep tropical convection

ACPD
10, 19469–19514, 2010

in different types of 3-D models, and to disentangle and quantify the relative role of convective transport on tracers' distribution in different models.

The general objective of this series of two papers is to assess the ability of models to represent tropical convection and to infer whether or not the convective transport of tracers and the resulting tracers' distributions are sufficiently well represented. We analyse results from different categories of models, such as CTMs, GCMs, and global and regional NWP models, and we attempt to attribute differences in convection and convective transport to differences in resolution, dynamics and convective parameterisations. The simulations used in these two papers where coordinated through a model intercomparison exercise under the European project SCOUT-O3 (http://www.ozone-sec.ch.cam.ac.uk/scout_o3/). Two rounds of model simulations were set up. In this paper we focus on the analysis of meteorological parameters (such as precipitation and cloud top height) that give an indication of the models ability to simulate the seasonal cycle, preferential locations, vertical extent and frequency of deep tropical convection. For this purpose we only used results from the second round of simulations since meteorological fields were not archived for the first round of simulations. The analysis of idealised tracers and the ability of models to provide realistic tracer transport in the Tropics are addressed in the second paper of this series (Hoyle et al., 2010). The two papers will focus on three main regions in the tropics, namely West Africa, the Maritime Continent and South America, which have been identified as having particularly strong convective activity, with clouds occasionally penetrating the lower stratosphere.

In this paper tropical convection characteristics are studied using observations for the year 2005. We use remote sensing observations from satellite platforms, since they provide a wider temporal and spatial coverage than in-situ measurements. We use more than one observational dataset for each variable in order to assess inherent differences between instruments and platforms and to provide a rough measure of the uncertainties in the observations. The comparison of observed convective properties with model results provides a useful benchmark to test model performance and

ACPD
10, 19469–19514, 2010

assess which characteristics of tropical convection are well captured and which ones are not. Because of the large number of observational datasets used (some with high temporal resolution and requiring further processing), and also due to the high computational cost of high resolution model runs, we focus our analysis on a single year. The year 2005 was chosen since measurement campaigns were carried out in South America (February) and North Australia (November and December) which found significant evidence of convective systems reaching the lower stratosphere. Additionally, there was no strong ENSO signal for 2005.

Sect. 2 of this paper is devoted to the description of the different models and details of the simulation setups. The observational data used is presented in Sect. 3. The results are analysed in Sect. 4. Conclusions are given in Sect. 5.

2 Description of the model simulations

Different categories of 3-D models use different approaches to calculate tracer transport. CTMs use 3-D wind fields from an independent model, usually operational analyses and/or forecasts, to perform large scale transport (also known as advection). For these models the fast vertical transport by deep convection can be either diagnosed from the convective fluxes provided by the independent model or recalculated by the CTM's own convective parameterisation scheme. GCMs and NWP models both use their own dynamical core to calculate 3-D wind fields and the resulting large scale transport. A chemistry scheme can be coupled to a GCM or NWP model to provide a Chemistry Climate Model (CCM) or an air-pollution forecast model. In this case, convective mass fluxes of chemical species are calculated by the model's convective parameterisation scheme.

Some of the models in this study use ECMWF operational analyses and/or forecasts, either to provide direct forcing for tracer transport (i.e. for CTMs), or to relax the model's meteorological fields to the analyses (a technique known as "nudging"). The limited area model in this study also uses ECMWF analyses to constrain the model's meteorology at the lateral boundary and at the model top.

ACPD
10, 19469–19514, 2010

In Table 1 we summarize the main features and also differences and similarities in the treatment of convection for the models participating in the second round of the intercomparison exercise. A brief description of the different models follows (for more details the reader is referred to the relevant literature).

Oslo-CTM2 (Berntsen et al., 2006) is a global chemistry-transport model. It has 40 vertical levels, with hybrid σ-p coordinates from surface to 2 hPa (~43 km). The horizontal resolution is ~2.8° longitude by ~2.8° latitude (T42 truncation). The model uses 3-hourly dynamic, thermodynamical and microphysical fields from forecasts run with ECMWF IFS model (cycle 29) and truncated at T42 resolution. Surface precipitation rates are output directly from ECMWF IFS forecasts, while cloud top heights are derived from ECMWF mass flux.

FRSGC-UCI CTM (Wild et al., 2003) has a very similar configuration to Oslo-CTM2 except that the lowest 5 model levels are merged into 2, resulting in a total of 37 vertical layers. Further differences between the two models exist on tracer transport and chemistry and are detailed in the second paper of this series. Since Oslo-CTM2 and FRSGC-UCI CTM use the same meteorological information, we analyse results from the two models together in this paper.

TOMCAT (Chipperfield 2006) is a Chemistry Transport Model. It has 31 vertical levels, with hybrid σ-p coordinates from surface to 10 hPa (~31 km). The horizontal resolution used in this study is the same as the other CTMs, ~2.8° longitude by ~2.8° latitude (T42 truncation). The model is forced by 6-hourly ECMWF operational analyses truncated at T42 resolution. Precipitation rates and cloud top heights are diagnosed by the model convective parameterisation scheme (Stockwell and Chipperfield, 1999) based on Tiedke 1989.

pTOMCAT (O'Connor et al., 2005) is a CTM with a very similar configuration to TOMCAT. Further differences between the two models exist on tracer transport and chemistry and are detailed in the second paper of this series. Since the meteorological fields from TOMCAT and pTOMCAT are virtually identical, we analyse the results together in this paper. Additionally, we show results from pTOMCAT_tropical, a modified version of

Discussion Paper | Discussion Paper | Discussion Paper | Discussion Paper |

ACPD

10, 19469–19514, 2010

pTOMCAT which has the same horizontal and vertical resolution but has been developed specifically for better representation of transport in tropical regions (see Barret et al., 2010). The main changes to the code are summarised as follows: surface moisture used to trigger convective clouds is derived from ISCCP cloud fractions (Rossow et al., 1996); entrainment rates for the convective column are set to half the value originally suggested by Tiedke et al. (1989); detrainment rates are set to zero, except at the top of the convective column.

UMUKCA-UCAM_nud (Telford et al., 2008) and UM-UCAM_highres (Petch et al., 2007; Hosking et al., 2010) are based on the UKMO Unified Model (UM). The model is non-hydrostatic with a hybrid σ-height vertical coordinate and 38 levels from the surface to 39 km. Shallow and deep convection are parameterised with a convective scheme by Gregory and Rowntree (1990). Sea surface temperatures and sea ice derived from the GISST 2.0 climatology (Parker et al., 1995) are used to constrain the model at the sea surface. The main difference between the two model configurations is the horizontal resolution, the former having a grid spacing of $3.75^{\circ} \times 2.5^{\circ}$ (N48), and the latter with a grid spacing of $0.83^{\circ} \times 0.56^{\circ}$ (N216). A "nudging" technique is applied to the coarser resolution configuration, whereby temperature and horizontal winds are relaxed to 6-hourly ECMWF analyses (Telford et al., 2008). The higher resolution configuration, being more computationally expensive, was only run for 4 time-slices of 1 month each, with initial conditions from UKMO operational analyses.

WRF version 3.1.1 (Skamarock et al., 2008) is a global NWP model. In this study the model configuration has 38 vertical levels, with a terrain-following hydrostatic-pressure vertical coordinate system from surface to 5 hPa (~37 km). The horizontal resolution is $1.87^{\circ} \times 1.25^{\circ}$ (N96). The model initial condition is derived from ECMWF analyses. The surface and boundary layer were represented using the quasi-normal scale elimination (QNSE) parameterisation scheme by Sukoriansky et al. (2005). Sub-grid scale effects of convective and shallow clouds are parameterised using the Betts-Miller-Janjic (BMJ) cumulus scheme (Janjic, 1994, 2000). The non-resolved convective transport of tracers is parameterised using an elevator approach based on the convective mass

ACPD
10, 19469–19514, 2010

flux through the atmospheric column.

CATT-BRAMS (Freitas et al., 2009) is a non-hydrostatic limited area model. The grid spacing is $0.5^{\circ} \times 0.5^{\circ}$ with 39 vertical levels from surface to ~40 km. Shallow and deep convection are parameterised following the ensemble parameterisation described in Grell and Dévényi (2002). Sea surface temperatures are derived from satellite weekly analyses. Initial conditions are from ECMWF analyses and the model is relaxed at the lateral and top boundaries to ECMWF 6-hourly analyses. This model configuration was only run for 1 month with a domain centred on the Maritime Continent (20° S to 20° N, 90° W to 150° W).

3 Observational datasets

Several satellite products are used to analyse the seasonal variability of deep convection in the tropics and to evaluate model results. Satellite estimates are preferred to other types of data because they provide a global and consistent coverage over the whole simulation period (i.e. the whole 2005 year). The high spatial and temporal coverage also allows us to make statistical comparisons with model results (which can be difficult with more sparse campaign data). The data retrieval from satellite observation is a complex process, leading to uncertainties in the measurements. Since these uncertainties are often hard to quantify, we have used more than one satellite product for each of the meteorological variables under investigation, thus providing an indirect measure of the uncertainty range in the observations.

We use precipitation rates, outgoing longwave radiation (OLR), cloud top pressure (converted to cloud top height), and water vapour at 150 hPa, to infer convective activity and analyse the seasonality and preferred locations of tropical convection. We additionally focus on surface precipitation rates and cloud top height to assess how well current models can represent tropical convection characteristics such as spatial patterns and vertical extent. Water vapour and OLR were not used for comparison with model data since these diagnostic are not easily available from CTMs.

ACPD
10, 19469–19514, 2010

Modelling tropical convection: comparison with observations

M. R. Russo et al.

3.1 Surface precipitation rates

Analysis of surface precipitation rates is performed using monthly mean estimates. Several products based on different satellite data and/or retrieval approaches are available for 2005.

The first product used for our analysis is the TRMM (Tropical Rainfall Measuring Mission) 3A12 dataset. It is available as a monthly mean at $0.5^\circ \times 0.5^\circ$ resolution calculated from the 2A12 dataset. 2A12 provides instantaneous rainfall rates and the vertical structure of hydrometeors and latent heating based upon the nine channels of the TRMM microwave imager, TMI (Kummerow et al., 1998). The processing algorithm (Kummerow et al., 1996) is based upon a Bayesian approach that begins by establishing a large database of potential hydrometeor profiles and their computed brightness temperatures. This database is computed from cloud resolving model simulations.

The second product used for this analysis is the Global Precipitation Climatology Project (GPCP) dataset. We use the daily mean dataset (1DD) on a $1^\circ \times 1^\circ$ grid to compile monthly means. This approach is preferred to the use of the monthly mean dataset since the latter is only available on a $2.5^\circ \times 2.5^\circ$ grid. The 1DD uses a combination of quasi-global observational datasets that have desirable time/space coverage (Huffman et al., 2001). The datasets include geosynchronous-orbit infra-red brightness temperatures, low-orbit infra-red GOES Precipitation Index, TIROS Operational Vertical Sounder (TOVS) and Atmospheric Infrared Sounder (AIRS). Although microwave precipitation estimates and gauge analyses are not explicitly used due to sampling limitations, the calibration of the 1DD to the monthly GPCP product ensures that they do have a strong influence on the overall scaling.

The third dataset is from the National Oceanic and Atmospheric Administration (NOAA) Climate Prediction Center (CPC) Merged Analysis of Precipitation, CMAP. It uses a technique which produces monthly analyses of global precipitation in which observations from raingauges are merged with precipitation estimates from several satellite-based algorithms (infrared and microwave). It uses values obtained from five

ACPD
10, 19469–19514, 2010

kinds of satellite estimates (GPI Global Precipitation Index, OPI outgoing-longwave radiation precipitation index, Special Sensor Microwave Imager SSM/I scattering, SSM/I emission and Microwave Sounding Unit MSU). The analyses are on a $2.5^{\circ} \times 2.5^{\circ}$ grid. The merging technique is thoroughly described in Xie and Arkin (1997).

3.2 Cloud top pressure/height

For the analysis of Cloud properties we use cloud top pressure from 3 datasets.

The first dataset is the D1 product from the International Satellite Cloud Climatology Project, ISSCP (Rossow and Schiffer, 1991; Rossow et al., 1993). ISCCP has been collecting, since July 1983, the infrared and visible radiances obtained from imaging radiometers carried on the international constellation of weather satellites. The analysis is composed of two major procedures: the cloud detection procedure divides the radiances into cloudy and clear groups and the radiative analysis procedure retrieves physical properties of clouds and the surface, respectively. For each individual pixel, either surface properties or cloud properties are retrieved from the pixel radiances depending on whether the threshold tests indicate clear or cloudy conditions. This creates the DX product. The D1 product is produced by combining the pixel-level results (DX data) every 3 h on an equal area map grid with 280 km or $\sim 2.5^{\circ}$, resolution and merging the results from separate satellites to produce global coverage at each time. One particular advantage of the ISCCP data is the high temporal resolution which allows sampling of the full diurnal cycle of convection.

The second and third datasets are from the MODerate resolution Imaging Spectroradiometer (MODIS) imagers on board the Terra and Aqua Earth Observing System (EOS) platforms (King et al., 2003). Unlike the ISCCP cloud climatology, the MODIS cloud data is collected from 2 sun-synchronous satellites, which sample cloud properties at 10:30 a.m./p.m. and 01:30 a.m./p.m. local time for EOS-Terra and EOS-Aqua, respectively. We use the Level-3 aggregated cloud top pressure provided daily on a 1° equal-angle grid. MODIS uses a CO_2 slicing technique (Wylie and Menzel, 1999) to evaluate cloud top pressure from radiances measured in spectral bands located within

Discussion Paper | Discussion Paper | Discussion Paper | Discussion Paper |

ACPD

10, 19469–19514, 2010

Modelling tropical convection: comparison with observations

M. R. Russo et al.

the broad 15-µm CO_2 absorption region. One advantage of this measurement technique is that cloud properties are derived similarly for both daytime and nighttime data as the IR method is independent of solar illumination. This approach is very useful for the analysis of mid-level to high-level clouds, and especially semi-transparent clouds such as cirrus.

Cloud top pressures were converted to cloud top heights using 6-hourly geopotential height from ECMWF analyses (interpolated to 3-hourly for the ISCCP dataset).

3.3 OLR

OLR data for the year 2005 is obtained from two datasets.

The first dataset is derived from radiances measured by the NOAA polar-orbiting satellites (Gruber and Krueger, 1984). The data, provided by the NOAA/OAR/ESRL PSD, is interpolated in space and time to eliminate missing values; the interpolation technique is described in Liebmann and Smith, 1996. We use monthly mean data, which is available globally on a 2.5° × 2.5° grid. The data is available from the NOAA website at http://www.esrl.noaa.gov/psd/.

The second dataset is from the Atmospheric Infrared Sounder AIRS onboard EOS-Aqua satellite. We use Level 3 Daily standard physical retrievals. AIRS is a high resolution spectrometer with 2378 bands in the thermal infrared and 4 bands in the visible. The OLR data has a global coverage, with a 1° × 1° grid-spacing. Daily values were averaged to produce monthly means.

3.4 Water vapour

Water vapour can be retrieved from different types of instruments but mainly in the troposphere where it is abundant. In the UTLS, because of the large vertical gradient and the very low values, water vapour measurements have large uncertainties.

The first dataset is obtained from the Microwave Limb Sounder (MLS) version 2.2, onboard EOS-Aura satellite (Sun-synchronous). MLS provides water vapour mixing

Discussion Paper | Discussion Paper | Discussion Paper | Discussion Paper |

ACPD

10, 19469–19514, 2010

Modelling tropical convection: comparison with observations

M. R. Russo et al.

ratios in the upper troposphere and stratosphere. Spatial coverage is nearly-global (−82° to +82° latitude), with each profile spaced 1.5° or ∼165 km along the orbit track (roughly 15 orbits per day). The recommended useful vertical range is between 316 and 0.002 hPa, and the vertical resolution is about 1.5 km at 316 hPa decreasing to 3.5 km to 4.6 hPa. The individual water vapour profiles were averaged on to a 5° × 5° grid at each pressure level to obtain monthly mean fields.

The second dataset is from the AIRS-Aqua measuring platform. The band ranges of the AIRS instrument have been specifically selected to allow determination of atmospheric humidity with an accuracy of 20% in layers 2 km thick in the troposphere. The AIRS/Aqua Level 3 Daily data has a global coverage, with a 1° × 1° grid-spacing, and the useful vertical range for water vapour is 1000–100 hPa. Daily values were averaged to produce monthly means.

4 Results

The seasonal and regional patterns of convection are illustrated in Fig. 1 for the southern and northern hemisphere summer season. This figure shows convective activity inferred by precipitation rates from the TRMM dataset. Among the areas where convection is strongest are the Maritime Continent in both seasons, South America in DJF and West Africa in JJA (highlighted with black boxes). Strong convection also occurs in other tropical regions, such as sub-equatorial Africa and the Tropical Warm Pool region. However we focus our modelling efforts on the three domains shown in Fig. 1, which have been the focus of extensive measurement campaigns aimed at understanding tropical convection, particularly its interactions with aerosols and chemical species, and its impact on transport of pollutants and water vapour to the UTLS (Pommereau et al., 2007; Vaughan et al., 2008; Cairo et al., 2010).

By choosing these three geographical domains, we are comparing areas where tropical convection has very different strength, seasonality and diurnal variation, and is also initiated by different mechanisms. The initial stages of cumulus convection are determined by soil moisture and other surface properties in Africa and South America,

ACPD
10, 19469–19514, 2010

while in a coastal and island domain, such as the Maritime Continent, sea breeze convergence is the main driver, with convection occurring preferentially over the hot land during the day and over the mild sea at night. Comparison of panels a and b in Fig. 1 highlights the strong seasonality of convection for Africa and South America, and to a lesser extent for the Maritime Continent region.

In order to understand the characteristics of tropical deep convection we start our analysis in Sect. 4.1, where we combine several observed variables to analyse the seasonal cycle of convection in the various regions; additionally, we investigate whether it is possible to find a correlation between water vapour measurements in the TTL and convective activity in order to assess the role of convection in the hydration or de-hydration of the TTL. The ability of models to reproduce the seasonal cycle of precipitation for different regions is also investigated.

In Sect. 4.2 monthly mean observations of surface precipitation rates and cloud top heights are compared to model data to assess the ability of models to reproduce the observed geographical distribution of convection. We discuss discrepancies between models and observations and try to attribute them to difference in model formulation, resolution, etc.

Surface precipitation rates and monthly mean cloud top heights can both be used to infer locations of strong convective activity. However, the information they provide cannot be used to directly estimate the vertical extent of convective systems. To investigate the impact of convective transport into the lower stratosphere we therefore need a measure of the height reached by tropical clouds and the frequency of occurrence of such high clouds; this will be discussed in Sect. 4.3.

4.1 Seasonal cycle of convection and its regional variations

The seasonal cycle of convection for the year 2005 is shown in detail in Fig. 2, where we analyse observed monthly mean fields averaged over the three domains of interest. This initial analysis is aimed at understanding how different variables, normally used as proxies for the strength of tropical convection, compare to each other. We then

ACPD
10, 19469–19514, 2010

compare the different domains to assess which ones have on average more convection, and how the strength of convection varies with the season.

For this analysis we use convective proxies such as surface precipitation rate (from TRMM, GPCP, CMAP), cloud top height (from MODIS-Terra and MODIS-Aqua) and OLR (from AIRS and NOAA); additionally, we plot water vapour at ~150 hPa (from AIRS and MLS) to investigate whether a correlation exists between water vapour concentration in the TTL and the strength of the convection. The use of different observational datasets for each of the analysed variables allows us to estimate the uncertainty range in the observations. In order to ascertain that our comparison of the three domains in question is not biased by the use of a single year of data, we also plot mean GPCP surface precipitation rates for the period 1979 to 2000. The comparison between precipitation rates for 2005 and the 20-year mean suggests that the convective behaviour (strength and seasonality) for the three domains in the year 2005 is not atypical.

Figure 2 highlights differences in the mean strength and seasonality of convection between the different domains. The seasonal cycle of precipitation rates (black lines) is more marked for Africa and South America, with distinctive maxima and minima, and less so for the Maritime Continent domain. West Africa has a maximum around July–August, while South America has a maximum in December–March. The Maritime Continent has a high background precipitation throughout the year, with a maximum in November–January. The lack of a marked minimum in the seasonal cycle for the Maritime Continent, compared to the other regions, is partly explained by the latitudinal range chosen for this domain (which lies more symmetrically across the Equator) and partly by differences in convective forcing. While convection in Africa and South America is modulated by large scale circulation processes with marked seasonal cycle (e.g. monsoons), convection occurring over the warm oceans and islands in the Tropics can be additionally driven by local processes (e.g. sea breezes) which are mostly influenced by the diurnal cycle. As a result, the tropical oceanic region between 90°–180° longitude receives a significant amount of rainfall throughout the year (as can be seen in Fig. 1).

ACPD
10, 19469–19514, 2010

Modelling tropical convection: comparison with observations

M. R. Russo et al.

The difference in precipitation rates between the three observational datasets (TRMM, GPCP and CMAP) is generally small for Africa and South America, with differences of about 15% and 5% respectively. In the Maritime Continent however, differences are on average around 30%. The differences between the datasets suggest that precipitation rates in the Maritime Continent are more uncertain and are more strongly affected by the choice of the observational data and possibly the horizontal resolution of the observations (TRMM being $0.5^\circ \times 0.5^\circ$ compared to $2.5^\circ \times 2.5^\circ$ for CMAP). We will expand on this analysis in Sect. 4.2.

While precipitation rates show the convective signal at the surface, OLR shows the convective signal at the top of the atmosphere. OLR is a complex variable and its value depends on the height of clouds, as well as temperature and water vapour concentrations at the convective outflow level. Despite its complexity, the seasonal cycle of OLR (cyan lines) mirrors closely that of precipitation, with minimum values where precipitation, and therefore convection, is highest and vice-versa. The two OLR datasets are in good agreement, except for a constant bias of around 10%, with AIRS showing consistently lower values (and therefore stronger convection) compared to NOAA. This discrepancy could be due to instrumental differences or to the different resolution of the dataset.

The mean cloud top heights (red lines) are derived from $1^\circ \times 1^\circ$ data using only gridpoints where the monthly mean is greater than zero (i.e. gridboxes which show no clouds in the monthly mean are not used in the spatial averaging). The two datasets are generally in good agreement, with differences of 5–10%. The ISCCP dataset was not used in this analysis because we only retrieved the 3-hourly data for selected months. The seasonal cycle of cloud top heights follows that of precipitation for the Maritime Continent and South America. However, it shows high values for West Africa throughout the year. Since precipitation rates are low and OLR values are high in the November to March period compared to August, we conclude that the high cloud top values observed for West Africa in this period could be due to problems in the detection and attribution of cloudy pixels over desert areas of Africa; this is supported by the

ACPD
10, 19469–19514, 2010

geographical distribution of monthly mean cloud top pressures, which show anomalously low values (high clouds) throughout the year for the Sahara desert, Greenland and Antarctica, which have higher than average surface albedos.

Comparing the seasonal cycle and relative strength of the convection for these three domains could help to understand which of these geographical areas has a greater impact on the UTLS composition, and at what time of year. In addition to the three domains shown in Fig. 2, we have performed a similar analysis for sub-equatorial Africa, [20 S:0; 0:40], which shows high precipitation rates in DJF (see Fig. 1). Analysis of the seasonal cycle for this region shows a maximum in January–March and a marked minimum in June–August; however the amplitude of the seasonal cycle and the maximum values for all convective proxies are very similar to those shown for West Africa, indicating that convection from this region would have a comparable effect to West Africa on the composition of the UTLS.

The analysis of convective activity for each of the domains in the year 2005, suggests that the relative strength of convection, inferred from the above variables, is greater for the Maritime Continent compared to the other tropical regions. From our analysis, the Maritime Continent is shown to have on average: higher precipitation rates of 8–10 mm/day in November–December, compared to 6–8 mm/day for South America in February–March and 4–5 mm/day for West Africa in July–August; higher cloud tops of 8–10 km compared to 6–7 km for the other two regions; similar OLR values to South America, 200–220 W/m^2, compared to 240–260 W/m^2 for West Africa. However, this analysis shows a monthly mean picture of convective properties averaged over a large domain and does not give an estimate of the relative strength and frequency of single convective events. The analysis in Sect. 4.3 will address this point by using highly temporally-resolved data and focusing on the month with the highest convective activity for each domain.

We now focus on the analysis of water vapour mixing ratio at 150 hPa (14–15 km). Water vapour can be thought of as a tropospherically-abundant tracer, with a marked vertical gradient and very small values in the UTLS; temperature-driven phase

ACPD
10, 19469–19514, 2010

transitions and removal through precipitating clouds however, make water vapour a complex tracer to assess convective transport. Water vapour in the stratosphere has a strong impact on the radiative budget of the atmosphere and therefore, despite its complexity as a tracer, understanding the links between the strength of tropical convection and the water vapour budget in the UTLS is crucial if we want to predict stratospheric feedbacks on surface temperature in a changing climate. The seasonal cycle from AIRS and MLS observations is shown in Fig. 2. The two water vapour products show similar variations but a nearly constant bias of about 30% for all considered regions. This bias is consistent with MLS validation studies by Read et al. (2007) and Lambert et al. (2007) based on comparisons with different datasets, including AIRS. Therefore we focus on the relative variations of water vapour with the season, rather than on the absolute concentrations. Firstly we analyse how the seasonal variation of the two water vapour datasets compare with each other: correlation of AIRS and MLS seasonal cycles is relatively high for West Africa and South America, where they correlate with a coefficient of 0.76 and 0.72, respectively; for the Maritime Continent, the seasonal variation of the two water vapour datasets shows larger differences, with a correlation coefficient of 0.52. Secondly we analyse how the seasonal variation for each of the water vapour datasets correlates with the seasonal variation of convection, as inferred by the different convective proxies (a similar analysis using only MLS water vapour data can be found in Liu 2007); the results can be summarized as follows. For South America both water vapour datasets correlate strongly with all other variables with a mean correlation coefficient of 0.86 and 0.80 for AIRS and MLS correlating respectively to all other datasets. For West Africa, AIRS correlates better to the other datasets compared to MLS, with correlation coefficients of 0.75 and 0.53, respectively. For the Maritime Continent AIRS correlates very poorly with other datasets, with a correlation coefficient of 0.12, while MLS has a better correlation, with a coefficient of 0.75. We can therefore conclude that for South America the net moistening of the TTL (at ~14–15 km) by deep convection is strongly supported by our analysis; for West Africa the correlation between moistening of the TTL and deep convection is less strong but still present in

Discussion Paper | Discussion Paper | Discussion Paper | Discussion Paper |

ACPD

10, 19469–19514, 2010

Modelling tropical convection: comparison with observations

M. R. Russo et al.

both water vapour datasets. For the Maritime Continent however, the moistening of the TTL by deep convection is supported by the MLS measurements of water vapour but not by AIRS. The discrepancy between the two datasets in the Maritime Continent region could be partly due to the challenges associated with the remote-sensing observation of water vapour; in particular, differences in the vertical resolution and vertical averaging of the two instruments can have a significant impact on water vapour measurements since the vertical gradients of water vapour in the UTLS are very large. Additionally, water vapour concentrations are also strongly influenced by temperature and its regional and seasonal variations: we therefore analysed the temperature distribution at 150 hPa from AIRS observations (not shown here) and found that the Maritime Continent region has colder temperatures (up to 1 degree difference) in the November to March period compared to other regions, suggesting that monthly mean water vapour concentrations in this period will be lower due to lower temperatures despite the strong convective activity. The water vapour analysis seems to indicate that deep convection can moisten the TTL through vertical transport of water from the free troposphere to up to 150 hPa (14–15 km). Unfortunately, the very low water vapour concentrations, large measurement uncertainties and colder temperatures at 100 hPa (16–17 km) make it more difficult to estimate the correlation between water vapour and convective activity at this height, since the strong temperature control would interfere with the convective transport of water vapour.

Finally, in Fig. 3 we compare the observed seasonal cycle of surface precipitation rates with model data to assess the models' ability to reproduce the observed seasonal variations for the different regions. In this analysis and most of the subsequent ones, some of the models are grouped together since their diagnosed field is either identical or very similar; this is the case for TOMCAT/pTOMCAT and OSLOCTM2/FRSGCUCI, which have very similar parameterisations for the meteorological fields. Figure 3 shows that for West Africa and South America all models can represent reasonably well the average strength and seasonality of convection (inferred from surface precipitation). For these two regions the models' precipitation rates are mostly within the range

ACPD
10, 19469–19514, 2010

provided by the observational data. However, the spread of model data is much larger for the Maritime Continent region, with some models greatly overestimating surface precipitation and others somewhat underestimating it. These results indicate that this set of models generally tends to better simulate continental precipitation and their well marked dry and wet season, while in a region like the Maritime Continent, some models fail to correctly represent the observed precipitation rates and their seasonal variations. In the next section we concentrate on these large model differences for the Maritime Continent region and try to understand their origin.

4.2 Assessment of model geographical distribution of convection

A better understanding of the models' discrepancies with observations in the Maritime Continent can be gained in this section by analysis of the geographical distribution of convection. We start by investigating the annual mean geographical distribution of surface precipitation rates for the year 2005, shown in Fig. 4. Most of the models represent reasonably well the geographical distribution of surface precipitation, which has a large annual signal for the Indian Ocean, the Maritime Continent, the Inter Tropical Convergence Zone (ITCZ), the South Pacific Convergence Zone (SPCZ) and South America, and a smaller signal for Africa. A few of the models tend to slightly overestimate the precipitation rates in the West Pacific. TOMCAT/pTOMCAT and pTOMCAT_tropical overestimate precipitation rates over large regions in the Tropics, particularly over the oceans; this is possibly due to the model's simplified method for calculating heat and moisture fluxes at the surface, which are then used to initiate convection. Convective events in these models are therefore more widespread and frequent over the ocean, producing large areas where mean precipitation rates are higher than observed.

Bearing in mind that the largest differences between observed and modelled precipitation rates occur in the Maritime Continent region (see Fig. 3 and Fig. 4), we now focus on the detailed analysis of convection in this area for the month of November. Figure 5 and 6 show respectively a comparison between observed and modelled precipitation rates and cloud top heights, for November 2005. The observed surface precipitation

ACPD
10, 19469–19514, 2010

rates show higher values over the large islands, in particular over the high orography of Borneo and New Guinea, and the Malaysian Peninsula; the precipitation enhancement over land is greatest in the TRMM data compared to the other datasets, and this is likely to be due to its higher resolution ($0.5^{\circ} \times 0.5^{\circ}$) which enables it to resolve smaller scale features. GPCP data, with a resolution of $1^{\circ} \times 1^{\circ}$, shows consistent maxima over the islands of Borneo and New Guinea, and the region around the Malaysian peninsula, although not quite as marked as TRMM. The preference for high precipitation values over land becomes less evident in the CMAP dataset, which has a coarse resolution of $2.5^{\circ} \times 2.5^{\circ}$. All the observed precipitation maps also show increased precipitation over some specific ocean areas, in particular south-west of Sumatra and north of New Guinea. In comparing modelled precipitation with observations, one should bear in mind that most of the models used in this paper have a low resolution which is similar to that of the CMAP dataset; exceptions are WRF, with a resolution closer to that of GPCP data, and UM-UCAM_highres and CATT-BRAMS, with a resolution very similar to TRMM data; we can therefore compare each model to the dataset having similar resolution. We will also focus our attention on the comparison of modelled and observed geographical patterns of precipitation rather than the actual precipitation values, since some models have biases in the mean precipitation rates which have been highlighted in Fig. 3. As can be expected, most of the coarse resolution models have a poor representation of the precipitation maxima over land areas. At a coarse resolution, similar to that used by most of the models in this study, the land-sea contrast in temperature and moisture, and surface characteristic such as coastlines and orography, are not well defined; consequently the formation of moisture rich sea-breezes, their inflow over the islands, and their interaction with orography, leading to enhanced precipitation, are not particularly well represented. This could explain the general lack of precipitation maxima in Borneo, New Guinea and the Malaysian peninsula region for most of the coarse resolution models, although OSLOCTM2/FRSGCUCI shows a local maximum over Borneo. With an intermediate resolution, WRF shows maxima over Borneo and Sumatra which are consistent with observations; it also produces

ACPD
10, 19469–19514, 2010

high precipitation rates in the proximity of New Guinea, although the rain intensities are high compared to the other maxima. UM-UCAM_highres correctly represents the location of precipitation maxima over land areas, although it overestimates intensities in New Guinea and Sumatra (and some of the smaller islands) and underestimates the intensities in the Malaysian peninsula. CATT-BRAMS shows a marked preference for precipitation over land, with good representation of the enhanced precipitation rates over New Guinea, although the intensity of the other land features is slightly underestimated. We now compare observed and modelled precipitation over ocean areas: the TOMCAT models tend to overestimate precipitation intensities (as discussed earlier); OSLOCTM2/FRSGCUCI show generally good agreement with only a slight underestimation of precipitation intensities south-west of Sumatra; UMUKCA-UCAM_nud shows generally good agreement except north of New Guinea and south-west of Sumatra (respectively overestimating and underestimating the precipitation intensities compared to other areas). WRF, UM-UCAM_highres and CATT-BRAMS generally underestimate the precipitation signal north of New Guinea; additionally, WRF has a large precipitation maximum in the oceanic region north of New Guinea, and CATT-BRAMS generally doesn't show precipitation rates above 4 mm/day for most oceanic regions); this seems to suggest that a higher model resolution does not necessarily result in an improvement on the location of oceanic precipitation. In summary, models with a coarse horizontal resolution generally fail to correctly represent the enhanced precipitation rates over the islands and peninsulas of the Maritime Continents; differences between observed and modelled precipitation rates over the ocean seem to be less sensitive to horizontal resolution and are harder to attribute, being affected by a combination of factors such as regional circulation patterns, moisture fluxes at the sea surface and microphysical parameterisation, which are represented differently in the different models. The difficulty for the current set of models to correctly represent the location and intensity of precipitation maxima over island and peninsulas, and the correct precipitation over oceanic regions, results in the Maritime Continent region showing large model discrepancies and large biases with respect to observations, as shown in Fig. 3.

ACPD
10, 19469–19514, 2010

To complement the information on the geographical distribution of convection inferred from precipitation rates, the distribution of mean cloud top heights for November 2005 is illustrated in Fig. 6. An estimate of the geographical distribution of mean cloud top heights is given for the three observational datasets on the top of Fig. 6. The horizontal resolution of these datasets is $2.5^{\circ} \times 2.5^{\circ}$ for ISCCP and $1^{\circ} \times 1^{\circ}$ for MODIS-Terra and MODIS-Aqua. The large bias between ISCCP and MODIS cloud top heights can be attributed to the different methods used to detect clouds: while the MODIS instrument is able to view the thin, persistent cirrus clouds (Wylie and Menzel, 1999) which are likely to originate at the convective outflow level, ISCCP estimates the properties of the radiatively effective cloud top. A study by Liao et al (Liao et al., 1995a, 1995b) shows that ISCCP tends to underestimate the height of clouds with diffuse tops, particularly frequent in the Tropics, and it also underestimates the fraction of high clouds since it fails to capture high level clouds with low optical thicknesses. This can explain why the two MODIS datasets have consistently higher mean cloud tops compared to ISCCP. The time sampling of the 3 datasets is also different: the monthly mean cloud heights are calculated from 3-hourly values for ISCCP, and from daily values for the two MODIS datasets, sampled respectively at 10:30 a.m./p.m. and 1:30 a.m./p.m. for MODIS-terra and MODIS-aqua. However, sub-sampling ISCCP cloud top data at similar times to the two MODIS datasets, showed just small differences in the vertical distribution of clouds (not shown here), with generally smaller fractions of high clouds when ISCCP data is sampled at similar times to MODIS-aqua, or MODIS-terra. We therefore assume that time sampling differences between the observational datasets have a small impact on the geographical distribution and mean values of cloud top heights for the Maritime Continent area. Despite the constant bias, the geographical distribution of convection (inferred from observed mean cloud top height) is very similar in the three observational datasets: mean cloud top heights are generally higher over land than over the sea, with maxima over the Malaysian peninsula, Sumatra, Borneo and New Guinea. The lack of high clouds in the ocean regions south west of Sumatra and north of New Guinea suggests that the local maxima shown over these areas in the monthly precipitation

ACPD
10, 19469–19514, 2010

Modelling tropical convection: comparison with observations

M. R. Russo et al.

datasets could be due to recurrent episodes of shallow convection. We now compare modelled cloud top heights to the observations: the main focus of this analysis is on assessing the models' ability to represent local maxima and minima rather than the mean value of cloud top height. Although we will try to explain model biases whenever possible, a more detailed comparison of modelled and observed vertical distribution of clouds is given in the next section.

Despite the fact that the coarse resolution models in this study failed to represent the maxima in precipitation associated with the Malaysian peninsula and Borneo, the maxima in cloud top height over the same areas are reasonably well reproduced by most models. However the coarse resolution models fail to correctly represent the maximum over New Guinea, both in the precipitation and cloud fields, and instead produce a maximum in precipitation and cloud top height over the ocean region north of New Guinea. One possible explanation for the unexpected ability of coarse resolution models to represent the maxima in cloud top height over the relatively large region covering the Malaysian peninsula, Sumatra and Borneo, while failing to capture the precipitation maxima in the same region is as follows: the coarse resolution models in this study are either CTMs using forcing from ECMWF analyses, or a nudged CCM using the same analyses to constrain its dynamical evolution; the height reached by convective clouds is less sensitive to the model's representation of surface features (such as coastlines and orography) compared to precipitation, and it is more sensitive to mid-level circulation and the vertical structure of the atmosphere, which are constrained to ECMWF analyses. For the relatively smaller New Guinea area, however, the analyses, which are degraded to the coarse resolution of the model, might not represent the location of the convective area appropriately. The WRF and UM-UCAM_highres models also show different locations for the maxima in precipitation and cloud top height, with both models showing a preference for high clouds over ocean areas which is not mirrored in the observations. CATT-BRAMS shows a consistent picture with marked maxima over land areas. The discrepancy between mean cloud top height and precipitation fields for some of the models suggests that the location of high clouds and

ACPD
10, 19469–19514, 2010

high precipitation rates are not always co-located. This is partly due to persistent shallow convection producing maxima in precipitation and not cloud height, and partly to the complex coupling of the deep convection parameterisation and cloud microphysical processes, which might not be adequately represented. Most of the models tend to show higher mean cloud top values compared to observations. This positive bias can be partly attributed to models generally underestimating fractions of mid-level clouds and slightly overestimating fractions of high-level clouds (Illingworth et al. 2007), which is also shown to be the case for most of the models in this study (not shown here). This discrepancy has in the past been attributed to convection schemes detraining too little moisture at mid levels and consequently detraining too much moisture at high levels. The widespread positive biases for the WRF model can be further explained by the underestimation of shallow convection in this region, which therefore pushes mean cloud top height values upwards; this is further supported by the short-lived (lifetime ~6 h) tracer profiles averaged over the Maritime Continent region (Hoyle et al 2010, Fig. 1) which shows that all other models have secondary peaks around 600–700 hPa associated with transport by shallow convection, while there is no such peak for the WRF model. In summary, the maxima in precipitation and cloud top height are not always co-located: coarse resolution models succeed in reproducing the maxima in cloud top height over the Malaysian peninsula, Sumatra and Borneo region but fail to reproduce the maxima in precipitation over the same region; over New Guinea, coarse resolution models fail to reproduce both maxima. Model biases in the mean value of cloud top heights are due to the overestimate of high clouds compared to mid-level and/or shallow clouds.

4.3 Assessment of model vertical distribution of clouds

We now attempt to evaluate the ability of models to reproduce the observed vertical distribution of clouds in the three highly convective regions of West Africa, the Maritime Continent and South America. We also use the observed vertical distribution of clouds to complement the results from Sect. 1 on the relative strength of convection in

ACPD
10, 19469–19514, 2010

the three domains under investigation. For each of the domains we use 3-hourly data (daily for MODIS) to calculate the percentage of grid points, over the domain and over one month, with cloud tops above a certain height. We show the results for clouds above 9–10 km which generally corresponds to the base of the TTL, and we focus specifically on clouds reaching the zero radiative heating level ($Q = 0$ level) which is estimated to be ∼15 km on average, or ∼14 km during daytime (Gettelmann et al., 2004). Clouds reaching the $Q = 0$ level can detrain surface species which can subsequently be transported upwards at an estimated rate of 0.1–0.2 K/day (Gettelmann et al., 2004) equivalent to ∼0.15–0.30 km/month. The fraction of clouds reaching this level should therefore give an indication of the relative impact of convection on the composition of the UTLS.

Analysis of Fig. 7 shows that ISCCP generally tends to underestimate mid- and high-level clouds compared to the MODIS datasets (the reasons for this discrepancy have been discussed in Sect. 4.2); MODIS-Aqua generally has the highest cloud values, except for the tail of the distribution (i.e. for clod tops above ∼16 km). The estimated vertical distributions of clouds from the three observational datasets are in better agreement for West Africa and South America, but show a larger discrepancy for the Maritime Continent; this might be due to different optical characteristics of clouds (i.e. more diffuse clouds), or to the larger fraction of cirrus clouds in this region compared to the other two (Liu 2007). The fraction of observed clouds with tops above 15 km is in the range 0.5–1.7% for the Maritime Continent, compared to 0.3–0.6% for West Africa and 0.2–0.9% for South America. The values from these convectively active regions can be compared to 0.1–0.2%, which is the fraction of observed clouds with tops above 15 km, calculated for a non convective region of the Atlantic ocean, [10 S:10 N; −40:0], over a period of three months (Febuary, August and November). This suggests that, for the months under investigation, 2 to 3 times more clouds reach the $Q = 0$ level in the Maritime Continent compared to West Africa and South America, while compared to a non-convective region in the Tropics, the Maritime Continent has up to ∼10 times more clouds reaching the $Q = 0$ level. To qualitatively extend this result on the annual

ACPD
10, 19469–19514, 2010

timescale, we can assume that the percentage of clouds reaching the $Q = 0$ level varies with the season according to the temporal evolution of convection shown in Fig. 2: convective activity and mean cloud top heights are generally high throughout the year for the Maritime Continent region, while West Africa and South America show marked minima in convective activity lasting 4 to 5 months. Therefore we expect fast vertical transport of surface species to the $Q = 0$ level to be more frequent and have a higher impact annually in the Maritime continent region compared to the other two regions.

Direct injection by overshooting convection is shown to be rare, at least according to this set of observations: the fraction of gridboxes having clouds above 16 km is at most 0.2% and often lower than 0.1% (depending on dataset and region); these values are in agreement with estimates from Liu and Zipser 2005. The percentage of clouds reaching above 16 km for the three domains are also relatively similar, indicating that there is not a strong regional preference for convection reaching above 16 km. Fast convective transport to the $Q = 0$ level (which is ∼10 times more frequent compared to direct injection above 16 km), followed by slow radiative ascent, can therefore provide an alternative pathway for short-lived halogenated species of surface origin into the tropical lower stratosphere. The lifetime of water-soluble species produced by oxidation of short-lived halocarbons can in fact be extended above the $Q = 0$ level thanks to low water vapour mixing ratios and reduced loss by wet-deposition. If this transport pathway was indeed effective for short-lived, biogenic halocarbons, such as bromoform and methyl-iodide, which are produced preferentially in the tropical coastal areas and shallow oceanic regions within the Maritime Continent, it could explain the discrepancy between the observed and modelled bromine mixing ratio in the tropical stratosphere (WMO Ozone Assessment Report, 2006).

When comparing modelled cloud vertical distributions with observations one should bear in mind that cloud top heights can be estimated from different model diagnostics (such as mass-flux, level of neutral buoyancy, cloud ice); cloud top heights from different models are therefore not always directly comparable. Additionally, models can have different approaches to simulate the vertical transport by convection, and they differ for

ACPD
10, 19469–19514, 2010

example in the values and height chosen for entrainment/detrainment; therefore the vertical extent of convective transport is not always directly related to the vertical distribution of clouds. Nevertheless, the analysis presented in this section provides a first-order comparison with observations and can additionally be used to interpret the differences in modelled convective transport (Hoyle et al., 2010).

The vertical distribution of mid- and high-level clouds in this set of models shows a wide range of values: TOMCAT/pTOMCAT underestimate the percentage of gridboxes with clouds tops above 12 km (or 13 km for West Africa), OSLOCTM2/FRSGCUCI, UMUKCA_UCAM_nud and, to a smaller extent, WRF tend to overestimate the percentage of gridboxes having clouds with tops above 13–14 km, while pTOMCAT_tropical, UM_UCAM_highres and CATT-BRAMS show cloud heights which are either slightly lower, or within the observed range, depending on the region. Although the vertical distribution of clouds for the higher resolution models is generally closer to the observed range, horizontal resolution is not a major factor in determining the vertical distribution of clouds: in fact pTOMCAT_tropical has a cloud distribution which is closer to observations compared to TOMCAT/pTOMCAT, despite having the same horizontal resolution and the same dynamical fields driving the large scale flow. A more detailed analysis of convection parameterisation in the TOMCAT model is currently under investigation (Feng et al., 2010). We now assess the ability of models to reproduce the relative strength of convection in the Maritime Continent compared to West Africa: OSLOCTM2/FRSGCUCI, UMUKCA_UCAM_nud, WRF and UM_UCAM_highres all show generally larger fractions of high-level clouds for the Maritime Continent compared to West Africa, which is consistent with observations; all the TOMCAT models however, show larger fractions of high clouds for West Africa compared to the Maritime Continent. In summary, there are generally large differences between the vertical distributions of clouds for the three observational datasets, this is partly due to ISCCP underestimating the fraction and height of high-level clouds, and is particularly obvious for the Maritime Continent region. Nevertheless, some models (e.g. TOMCAT/pTOMCAT) have significant negative biases compared to observations, and

ACPD
10, 19469–19514, 2010

others (e.g. OSLOCTM2/FRSGCUCI, and UMUKCA_UCAM_nud) have large positive biases. Analysis of the modelled vertical convective transport of tracers (Hoyle et al., 2010) shows that TOMCAT and pTOMCAT have significantly lower convective outflows compared to other models, which is in consistent with the lower cloud top heights compared to observations. Differences in the height of convective outflow between the other models however are small and they don't always reflect directly the modelled vertical distribution of cloud top heights.

5 Conclusions

We have analysed the seasonal cycle of convection for three tropical regions (namely West Africa, the Maritime Continent and South America) using a large number of observational datasets for the year 2005. The Maritime Continent shows consistently strong convection throughout the year and the information from monthly mean observations suggests that it has stronger convection compared to the other two regions. Models can reproduce reasonably well the seasonal cycle and observed values of precipitation rates for West Africa and South America, but generally fail to correctly represent monthly mean precipitation rates and their temporal evolution for the Maritime Continent region.

Analysis of the annual mean global maps of precipitation rates also show that models are in better agreement with observations over continental-scale land regions but show larger discrepancies over the islands, peninsulas and ocean regions of the Maritime Continent. Further analysis of the geographical distribution of convection for the Maritime Continent in November, shows that the observed preference for convection over land areas compared to ocean areas is not always correctly reproduced by models: the enhanced precipitation rates over the islands and peninsulas of the Maritime Continent are better represented by high resolution models. Some models tend to overestimate precipitation rates and cloud top heights over the ocean regions of the Maritime Continent, and these features seem to be less dependent on the horizontal resolution of the

ACPD
10, 19469–19514, 2010

models. The models' inability to correctly capture the land-sea differences in convective activity can have implications on transport whenever short-lived chemical species have large land-sea contrast in emissions or surface concentrations: this is the case for many important chemical species such as isoprene (emitted over tropical land regions), methyl-iodide and bromoform (emitted in shallow and warm oceanic regions).

The vertical distribution of clouds from three different observational datasets suggests that the Maritime Continent has the largest fraction of clouds reaching above the $Q = 0$ level compared to West Africa and South America. The percentage of clouds reaching above 16 km can be up to 10 times smaller compared to clouds reaching above the $Q = 0$ level. For short-lived species, the fast convective transport to the $Q = 0$ level, followed by radiative ascent, can provide an effective pathway to the tropical lower stratosphere.

Most models largely underestimate the fractions of mid-level clouds (3–6 km), with some additionally underestimating the fraction of clouds above 12 km and others overestimating the fraction of clouds above 13–14 km; however the observed model differences in cloud top heights are not always directly related to differences in the mean height of the convective transport and the latter will be addressed in Hoyle et al. (2010). The implications of these model biases for the chemistry budget of the UTLS will be largest for short-lived species, such as lightning NO_x, or methyl-iodide, which are most sensitive to fast convective transport due to their short lifetime. Both these chemical species are produced in tropical regions, either in the free troposphere by electrically-active convective storms, or at the ocean surface. Both species have the potential to greatly impact the ozone budget in the UTLS. Due to the large vertical gradient of ozone at the tropical tropopause, the correct representation of the height at which these species are detrained is therefore crucial for models to correctly predict their impact on UTLS ozone.

Acknowledgements. This work has been supported by the integrated European project SCOUT-O3. Model simulations of the UM, WRF and pTOMCAT models were performed on the HECToR UK national supercomputing facilities. Technical support for the UM model was

ACPD
10, 19469–19514, 2010

Modelling tropical convection: comparison with observations

M. R. Russo et al.

Title Page
Abstract | Introduction
Conclusions | References
Tables | Figures
◀| |▶
◀ ▶
Back | Close
Full Screen / Esc
Printer-friendly Version
Interactive Discussion

provided by NCAS-CMS. The CATT-BRAMS work was supported by the program LEFE/INSU in France (projects UTLS-tropicale and Tropopause 2009) and was performed using HPC resources of CINES under the allocation 2008 – c2008012536 and 2009 – c2009015036 made by GENCI (Grand Equipement National de Calcul Intensif). We thank NASA for the TRMM, GPCP, ISCCP, MODIS, AURA-MLS, and AIRS datasets. We thank NOAA for providing CMAP and NOAA OLR datasets.

References

Adler, R. F., Huffman, G. J., Chang, A., Ferraro, R., Xie, P., Janowiak, J., Rudolf, B., Schneider, U., Curtis, S., Bolvin, D., Gruber, A., Susskind, J., Arkin, P., and Nelkin, E.: The Version 2 Global Precipitation Climatology Project (GPCP) Monthly Precipitation Analysis (1979–Present), J. Hydrometeor., 4, 1147–1167, 2003.

Alcala, C. M. and Dessler, A. E.: Observations of deep convection in the tropics using the Tropical Rainfall Measuring Mission (TRMM) precipitation radar, J. Geophys. Res., 107(D24), 4792, doi:10.1029/2002JD002457, 2002.

Arakawa, A. and Schubert, W. H.: Interaction of a cumulus cloud ensemble with the large-scale environment, Part I., J. Atmos. Sci., 31, 674–701, 1974.

Arteta, J., Marécal, V., and Rivière, E. D.: Regional modelling of tracer transport by tropical convection – Part 1: Sensitivity to convection parameterization, Atmos. Chem. Phys., 9, 7081–7100, doi:10.5194/acp-9-7081-2009, 2009.

Arteta, J., Marécal, V., and Rivière, E. D.: Regional modelling of tracer transport by tropical convection – Part 2: Sensitivity to model resolutions, Atmos. Chem. Phys., 9, 7101–7114, doi:10.5194/acp-9-7101-2009, 2009.

Barret, B., Williams, J. E., Bouarar, I., Yang, X., Josse, B., Law, K., Pham, M., Le Flochmoën, E., Liousse, C., Peuch, V. H., Carver, G. D., Pyle, J. A., Sauvage, B., van Velthoven, P., Schlager, H., Mari, C., and Cammas, J.-P.: Impact of West African Monsoon convective transport and lightning NO_x production upon the upper tropospheric composition: a multi-model study, Atmos. Chem. Phys., 10, 5719–5738, doi:10.5194/acp-10-5719-2010, 2010.

Berntsen, T., Fuflestvedt, Myhre, G., Stordal, F., and Berglen, T. F.: Abatement of greenhouse gases: does location matter?, Climatic Change, 74, 377–411, doi:10.1007/s10584-006-0433-4, 2006.

Berthet, G., Esler, J. G., and Haynes, P. H.: A Lagrangian perspective of the tropopause and the ventilation of the lowermost stratosphere, J. Geophys. Res., 112, D18102, doi:10.1029/2006JD008295, 2007.

Cairo, F., Pommereau, J. P., Law, K. S., Schlager, H., Garnier, A., Fierli, F., Ern, M., Streibel, M., Arabas, S., Borrmann, S., Berthelier, J. J., Blom, C., Christensen, T., D'Amato, F., Di Donfrancesco, G., Deshler, T., Diedhiou, A., Durry, G., Engelsen, O., Goutail, F., Harris, N. R. P., Kerstel, E. R. T., Khaykin, S., Konopka, P., Kylling, A., Larsen, N., Lebel, T., Liu, X., MacKenzie, A. R., Nielsen, J., Oulanowski, A., Parker, D. J., Pelon, J., Polcher, J., Pyle, J. A., Ravegnani, F., Rivière, E. D., Robinson, A. D., Röckmann, T., Schiller, C., Simões, F., Stefanutti, L., Stroh, F., Some, L., Siegmund, P., Sitnikov, N., Vernier, J. P., Volk, C. M., Voigt, C., von Hobe, M., Viciani, S., and Yushkov, V.: An introduction to the SCOUT-AMMA stratospheric aircraft, balloons and sondes campaign in West Africa, August 2006: rationale and roadmap, Atmos. Chem. Phys., 10, 2237–2256, doi:10.5194/acp-10-2237-2010, 2010.

Chemel, C., Russo, M. R., Pyle, J. A., Sokhi, R. S., and Schiller, C.: Quantifying the Imprint of a Severe Hector Thunderstorm during ACTIVE/SCOUT-O3 onto the Water Content in the Upper Troposphere/Lower Stratosphere, Mon. Weather Rev., 137(8), 2493–2514, 2009.

Dequé, M., Dreveton, C., Braun, A., and Cariolle, D.: The ARPEGE/IFS atmosphere model: a contribution to the French community climate modelling, Clim. Dyn., 10, 249–266, 1994.

Feng, W., Chipperfield, M. P., Dhomse, S., Monge-Sanz, B., and Yang, X.: Evaluation of cloud convection and tracer transport in a three-dimensional chemical transport model, Atmos. Chem. Phys. Discuss., in preparation, 2010.

Folkins, I., Loewenstein, M. Podolske, J., Oltmans, S. J., and Proffitt, M.: A barrier to vertical mixing at 14 km in the tropics: evidence from ozonesondes and aircraft measurements, J. Geophys. Res., 104, D18, 22095–22102, 1999.

Freitas, S. R., Longo, K. M., Silva Dias, M. A. F., Chatfield, R., Silva Dias, P., Artaxo, P., Andreae, M. O., Grell, G., Rodrigues, L. F., Fazenda, A., and Panetta, J.: The Coupled Aerosol and Tracer Transport model to the Brazilian developments on the Regional Atmospheric Modeling System (CATT-BRAMS) – Part 1: Model description and evaluation, Atmos. Chem. Phys., 9, 2843–2861, doi:10.5194/acp-9-2843-2009, 2009.

Fueglistaler, S., Wernli, H., and Peter, T.: Tropical troposphere-to-stratosphere transport inferred from trajectory calculations, J. Geophys. Res., 109, D03108, doi:10.1029/2003JD004069, 2004.

Fueglistaler, S., Dessler, A., Dunkerton, T. J., Folkins, I., Fu, Q., and Mote, P. W.: The tropical

tropopause layer, Rev. Geophys., 47, RG1004, doi:10.1029/2008RG000267, 2009.
Gettelman, A. and de F. Forster, P. M.: A climatology of the tropical tropopause layer, J. Met. Soc. Jpn., 80, 911–942, 2002.
Gettelman, A., Salby, M. L., and Sassi, F.: The distribution and influence of convection in the tropical tropopause region, J. Geophys. Res., 107, 2002.
Gettelmann A., de F. Forster, P. M., Fujiwara, M., Fu, O., Vömel, H., Gohar, L. K., Johanson, C., and Ammerman, M.: Radiation balance of the tropical tropopause layer, J. Geophys. Res., 109, D07103, doi:10.1029/2003JD004190, 2004.
Gregory, D. and Rowntree, P.: A mass flux convection scheme with representation of cloud ensemble characteristics and stability-dependent closure, Mon. Weather Rev., 118, 1483–1506, 1990.
Grell, G. A.: Prognostic evaluation of assumptions used by cumulus parameterizations, Mon. Weather Rev., 121, 764–787, 1993.
Grell, G. A. and Dévényi, D.: A generalized approach to parameterizing convection combining ensemble and data assimilation, Geophys. Res. Lett., 29, 1693, doi:10.1029/2002GL015311, 2002.
Grosvenor, D. P., Choularton, T. W., Coe, H., and Held, G.: A study of the effect of overshooting deep convection on the water content of the TTL and lower stratosphere from Cloud Resolving Model simulations, Atmos. Chem. Phys., 7, 4977–5002, doi:10.5194/acp-7-4977-2007, 2007.
Gruber, A. and Krueger, A. F.: The status of NOAA outgoing longwave radiation data set, B. Am. Meteor. Soc., 65, 958–962, 1984.
Highwood, E. J. and Hoskins, B. J.: The tropical tropopause, Q. J. Roy. Meteorol. Soc., 124, 1579–1604, 1998.
Hosking, J. S., Russo, M. R., Braesicke, P., and Pyle, J. A.: Modelling deep convection and its impacts on the tropical tropopause layer, Atmos. Chem. Phys. Discuss., in review, 2010.
Hoyle, C. R., Marécal, V., Russo, M. R., Arteta, J., Chemel, C., Chipperfield, M. P., D'Amato, F., Dessens, O., Feng, W., Harris, N. R. P., Hosking, J. S., Morgenstern, O., Peter, T., Pyle, J. A., Reddmann, T., Richards, N. A. D., Telford, P. J., Tian, W., Viciani, S., Wild, O., Yang, X., and Zeng, G.:Tropical deep convection and its impact on composition in global and mesoscale models, Part 2: Tracer transport, Atmos. Chem. Phys. Discuss., submitted, 2010.
Huffman, G. J., Adler, R. F., Morrissey, M., Bolvin, D. T., Curtis, S., Joyce, R., McGavock, B., and Susskind, J.: Global precipitation at one-degree daily resolution from multi-satellite

observations, J. Hydrometeor., 2, 36–50, 2001.

Illingworth, A. J., Hogan, R. J., O'Connor, E. J., et al.: Cloudnet: Continuous evaluation of cloud profiles in seven operational models using ground-based observations, B. Am. Meteor. Soc., 88, 883–898, 2007.

Janjic, Z.: The Step-Mountain ETA Coordinate model – further developments of the convection, viscous sublayer, and turbulence closure schemes, Monthly Weather Review, 122, 927–945, 1994.

Janjic, Z.: Comments on "Development and evaluation of a convection scheme for use in climate models", J. Atmos. Sci., 57, p. 3686, 2000.

Kain, J. S. and Fritsch, J. M.: A one-dimensional entraining/detraining plume model and its application in convective parameterization, J. Atmos. Sci., 47, 2784–2802, 1990.

King, M. D., Menzel, W. P., Kaufman, Y. J., Tanre, D., Gao, B. C., Platnick, S., Ackerman, S. A., Remer, L. A., Pincus, R., and Hubanks, P. A.: Cloud and aerosol properties, precipitable water, and profiles of temperature and water vapor from MODIS, IEEE Trans. Geo. Rem. Sens., 41, 442–458, 2003.

Kummerow, C. , Barnes, W., Kozu, T., Shiue, J., and Simpson, J.: The Tropical Rainfall Measuring Mission (TRMM) Sensor Package, J. Atmos. Ocean Tech., 15, 808–816, 1998.

Kummerow, C., Olson, W. S. and Giglio, L.: A Simplified Scheme for Obtaining Precipitation and Vertical Hydrometeor Profiles from Passive Microwave Sensors, IEEE T. Geosci. Remote, 34, 1213–1232, 1996.

Lawrence, M. G. and Rasch, P. J.: Tracer transport in deep convective updrafts: plume ensemble versus bulk formulations, J. Atmos. Sci., 62, 2880–2894, 2005.

Levine, J. G., Braesicke, P., Harris, N. R. P., Savage, N. H., and Pyle, J., A.: Pathways and timescales for tropospherето-stratosphere transport via the tropical tropopause layer and their relevance for very short lived substances, J. Geophys. Res., 112, D04308, doi:10.1029/2005JD006940, 2007.

Liao, X., Rind, D., and Rossow, W. B.: Comparison between SAGE II and ISCCP high-level clouds, Part I: Global and zonal mean cloud amounts, J. Geophys. Res., 100, 1121–1135, 1995.

Liao, X., Rind, D., and Rossow, W. B.: Comparison between SAGE II and ISCCP high-level clouds, Part II: Locating cloud tops, J. Geophys. Res., 100, 1137–1147, 1995.

Liebmann, B. and Smith, C. A.: Description of a Complete (Interpolated) Outgoing Longwave Radiation Dataset, B. Am. Meteor. Soc., 77, 1275–1277, 1996.

ACPD

10, 19469–19514, 2010

Modelling tropical convection: comparison with observations

M. R. Russo et al.

Liu, C. and Zipser, E. J.: Global distribution of convection penetrating the tropical tropopause, J. Geophys. Res., 110, D23104, doi:10.1029/2005JD006063, 2005.

Liu, C. T.: Geographical and seasonal distribution of tropical tropopause thin clouds and their relation to deep convection and water vapor viewed from satellite measurements, J. Geophys. Res.-Atmos., 112, D09205, doi:10.1029/2006JD007479, 2007.

Mapes, B. E., Warner, T. T., XU, M., and Gochis, D. J.: Comparison of cumulus parameterizations and entrainment using domain-mean wind divergence ain a regional model, J. Atmos. Sci., 61, 1284–1295, 2004.

Marécal, V., Rivière, E. D., Held, G., Cautenet, S., and Freitas, S.: Modelling study of the impact of deep convection on the utls air composition – Part I: Analysis of ozone precursors, Atmos. Chem. Phys., 6, 1567–1584, doi:10.5194/acp-6-1567-2006, 2006.

Parker, D., Jackson, M., and Horton, E.: The 1961–1990 GISST2.2 sea surface temperature and sea ice climatology, Tech. rep., Climate Research Technical Note N°63, 1995.

Petch, J., Willet, M., Wong, R. and Woolnough, S.: Modelling suppressed and active convection. Comparing a numerical weather prediction, cloud-resolving and single-column model, Q. J. Roy. Meteorol. Soc., 133, 1,807-1,100, 2007.

Pickering, K. E., Thompson, A. M., Wang, Y., Tao, W.-K., McNamara, D. P., Kirchhoff, V. W. J. H., Heikes, B. G., Sachse, G. W., Bradshaw, J. D., Gregory, G. L., and Blake, D. R.: Convective transport of biomass burning emissions over Brazil during TRACE A, J. Geophys. Res., 101(D19), 23993–24012, 1996.

Pommereau, J.-P., Garnier, A., Held, G., Gomes, A.-M., Goutail, F., Durry, G., Borchi, F., Hauchecorne, A., Montoux, N., Cocquerez, P., Letrenne, G., Vial, F., Hertzog, A., Legras, B., Pisso, I., Pyle, J. A., Harris, N. R. P., Jones, R. L., Robinson, A., Hansford, G., Eden, L., Gardiner, T., Swann, N., Knudsen, B., Larsen, N., Nielsen, J., Christensen, T., Cairo, F., Pirre, M., Marécal, V., Huret, N., Riviére, E., Coe, H., Grosvenor, D., Edvarsen, K., Di Donfrancesco, G., Ricaud, P., Berthelier, J.-J., Godefroy, M., Seran, E., Longo, K., and Freitas, S.: An overview of the HIBISCUS campaign, Atmos. Chem. Phys. Discuss., 7, 2389–2475, doi:10.5194/acpd-7-2389-2007, 2007.

Pope, V. D., Pamment, J. A., Jackson, D. R., and Slingo, A.: The representation of water and its dependence on vertical resolution in the Hadley Centre climate model, J. Climate, 14, 3065–3085, 2001.

Rossow, W. B. and Schiffer, R. A.: ISCCP Cloud Data Products, B. Am. Meteor. Soc., 72, 2–20, 1991.

Rossow, W. B., Walker, A. W., and Garder, L. C.: Comparison of ISCCP and Other Cloud Amounts, J. Clim., 6, 2394–2418, 1993.
Rossow, W. B., Walker, A. W., Beuschel, D. E., and Roiter, M. D.: International Satellite Cloud Climatology Project (ISCCP) Documentation of New Cloud Datasets, WMO/TD-No. 737, World Meteorological Organization, 115 pp., 1996.
Rossow, W. B. and Pearl, C.: 22-Year survey of tropical convection penetrating into the lower stratosphere, Geophys. Res. Lett., 34, L04803, doi:10.1029/2006GL028635, 2007.
Ricaud, P., Barret, B., Attié, J.-L., Motte, E., Le Flochmoën, E., Teyssèdre, H., Peuch, V.-H., Livesey, N., Lambert, A., and Pommereau, J.-P.: Impact of land convection on troposphere-stratosphere exchange in the tropics, Atmos. Chem. Phys., 7, 5639–5657, doi:10.5194/acp-7-5639-2007, 2007.
Rind, D.: Dependence of warm and cold climate depiction on climate model resolution, J. Clim., 1, 965–997, 1988.
Schiller, C., Grooß, J.-U., Konopka, P., Plöger, F., Silva dos Santos, F. H., and Spelten, N.: Hydration and dehydration at the tropical tropopause, Atmos. Chem. Phys., 9, 9647–9660, doi:10.5194/acp-9-9647-2009, 2009.
Skamarock, W. C., Klemp, J. B., Dudhia, J., Gill, D. O., Barker, D. M., Duda, M. G., Huang, X.-Y., Wang, W., and Powers, J. G.: A description of the Advanced Research WRF Version 3, NCAR Technical Note, NCAR/TN-475+STR, NCAR, Boulder, CO, USA, 125 pp., 2008.
Sherwood, S. C. and Dessler, A. E.: A model for transport across the tropical tropopause, J. Atmos. Sci., 58, 765–779, 2001.
Skamarock, W. C., Klemp, J. B., Dudhia, J., Gill, D. O., Barker, D. M., Duda, M. G., Huang, X.-Y., Wang, W., and Powers, J. G.: A description of the Advanced Research WRF Version 3, NCAR Technical Note NCAR/TN-475+STR, NCAR, NCAR Boulder, CO, USA, 2008.
Sukoriansky, S., Galperin, B., and Staroselsky, I.: A quasinormal scale elimination model of turbulent flows with stable stratification, Phys. Fluids, 17, 085107, doi:10.1063/1.2009010, 2005.
Telford, P. J., Braesicke, P., Morgenstern, O., and Pyle, J. A.: Technical Note: Description and assessment of a nudged version of the new dynamics Unified Model, Atmos. Chem. Phys., 8, 1701–1712, doi:10.5194/acp-8-1701-2008, 2008.
Tiedke, M.: A comprehensive mass flux scheme for cumulus parameterization in large scale models, Mon. Weather Rev., 117, 1779–1800, 1989.
Tost, H., Lawrence, M. G., Brühl, C., Jöckel, P., The GABRIEL Team, and The SCOUT-O3-

ACPD
10, 19469–19514, 2010

Modelling tropical convection: comparison with observations

M. R. Russo et al.

DARWIN/ACTIVE Team: Uncertainties in atmospheric chemistry modelling due to convection parameterisations and subsequent scavenging, Atmos. Chem. Phys., 10, 1931–1951, doi:10.5194/acp-10-1931-2010, 2010.

Vaughan, G., Schiller, C., MacKenzie, A. R., Bower, K., Peter, T., Schlager, H., Harris, N. R. P., and May, P. T.: SCOUTO3/ACTIVE: High-altitude Aircraft Measurements around Deep Tropical Convection, B. Am. Meteorol. Soc., 89, 647–662, 2008.

Walko, R. L., Cotton, W. R., Meyers, M. P. and Harrington, J. Y.: New RAMS cloud microphysics parameterization. Part I: The single-moment scheme, 38, 29–62, 1995.

Wild, O., Sundet, J. K., Prather, M. J., Isaksen, S. A., Akimoto, H., Browell, E. V., and Oltmans, S. J.: Chemical transport model ozone simulations for spring 2001 over the western Pacific: Comparisons with TRACE-P lidar, ozonesondes and Total Ozone Mapping Spectrometer columns, J. Geophys. Res., 108(D21), 8826, doi:10.1029/2002JD003283, 2003.

WMO (World Meteorological Organization): Scientific Assessment of Ozone Depletion: 2006, Global Ozone Research and Monitoring Project Report No. 50, Geneva, Switzerland, 2007.

Wylie, D. P. and Menzel, W. P.: Eight years of global high cloud statistics using HIRS, J. Climate., 12, 170–184, 1999.

Xie, P. and Arkin, P. A.: Global precipitation: A 17-year monthly analysis based on gauge observations, satellite estimates, and numerical model outputs, B. Am. Meteor. Soc., 78, 2539–2558, 1997.

Yano, J.-I.: Deep-convective vertical transport: what is mass flux?, Atmos. Chem. Phys. Discuss., 9, 3535–3553, doi:10.5194/acpd-9-3535-2009, 2009.

Zhang, G. J. and McFarlane, N. A.: Sensitivity of climate simulations to the parameterization of cumulus convection in the Canadian Climate Centre General Circulation Model, Atmos. Ocean., 33, 407–446, 1995.

ACPD

10, 19469–19514, 2010

Modelling tropical convection: comparison with observations

M. R. Russo et al.

Table 1. Description of model configurations and setup.

Model Name	Model Category	Resolution: Horizontal; n vertical levels	Dynamics	Nudging (if applied)	Simulation period	Convective parameterisation
OSLOCTM2	CTM-global	T42 ($\sim 2.8^\circ \times 2.8^\circ$) L40	Off-line ECMWF	N/A	2005 year	No
FRSGCUCI	CTM-global	T42 ($\sim 2.8^\circ \times 2.8^\circ$) L37	Off-line ECMWF	N/A	2005 year	No
TOMCAT	CTM-global	T42 ($\sim 2.8^\circ \times 2.8^\circ$) L31	Off-line ECMWF	N/A	2005 year	Tiedke (1989)
pTOMCAT	CTM-global	T42 ($\sim 2.8^\circ \times 2.8^\circ$) L31	Off-line ECMWF	N/A	2005 year	Tiedke (1989)
UMUKCA-UCAM_nud	GCM-global	N48 ($\sim 3.7^\circ \times 2.5^\circ$) L38	On-line	U, V and T from ECWMF	2005 year	Gregory and Rowntree (1990)
WRF	NWP-global	N96 ($\sim 1.9^\circ \times 1.2^\circ$) L38	On-line	No	2005 year	Janjic (1994, 2000)
UM-UCAM_highres	NWP-global	N216 ($0.8^\circ \times 0.5^\circ$) L38	On-line	No	2005: Feb, May, Aug and Nov	Gregory and Rowntree (1990)
CATT-BRAMS	NWP-regional	($0.5^\circ \times 0.5^\circ$) L38	On-line	Lat. Boundary: U, V, T and Q from ECMWF	2005 Nov	Grell and Dévényi (2002)

ACPD
10, 19469–19514, 2010

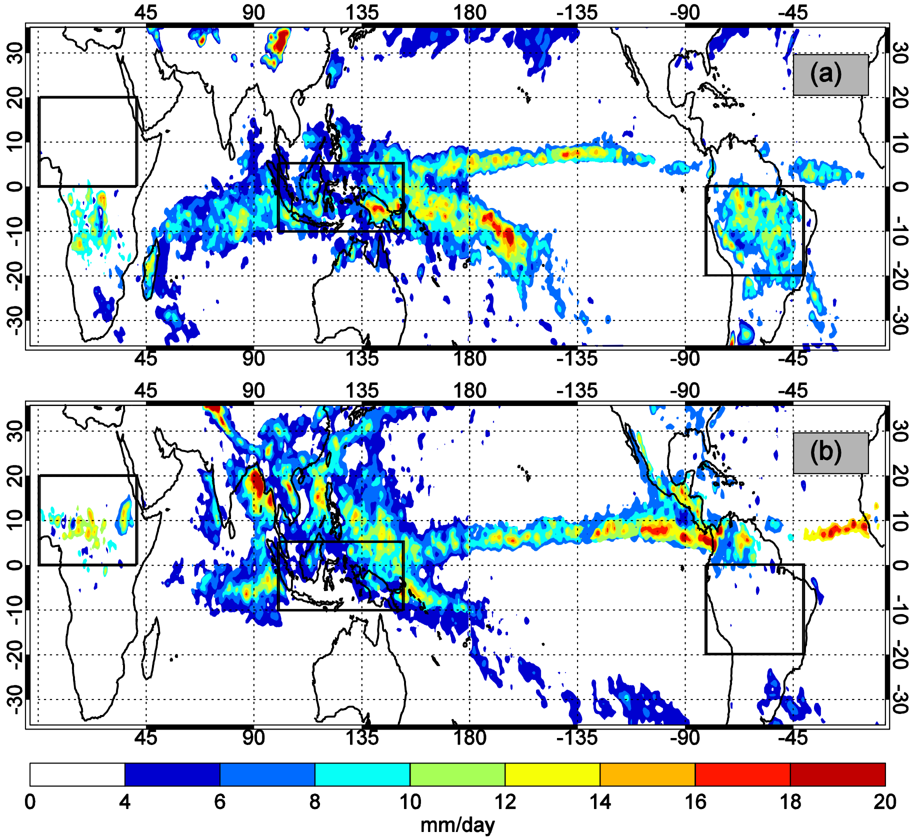

Fig. 1. Mean precipitation rates from TRMM dataset for the year 2005: **(a)** DJF, **(b)** JJA. The black boxes identify domains under investigation, namely West Africa (0:20° N; 0:40°), the Maritime Continent (–10° S:5° N; 100°:150°), and South America (–20° S:0°; –80°:–40°).

ACPD
10, 19469–19514, 2010

Modelling tropical convection: comparison with observations

M. R. Russo et al.

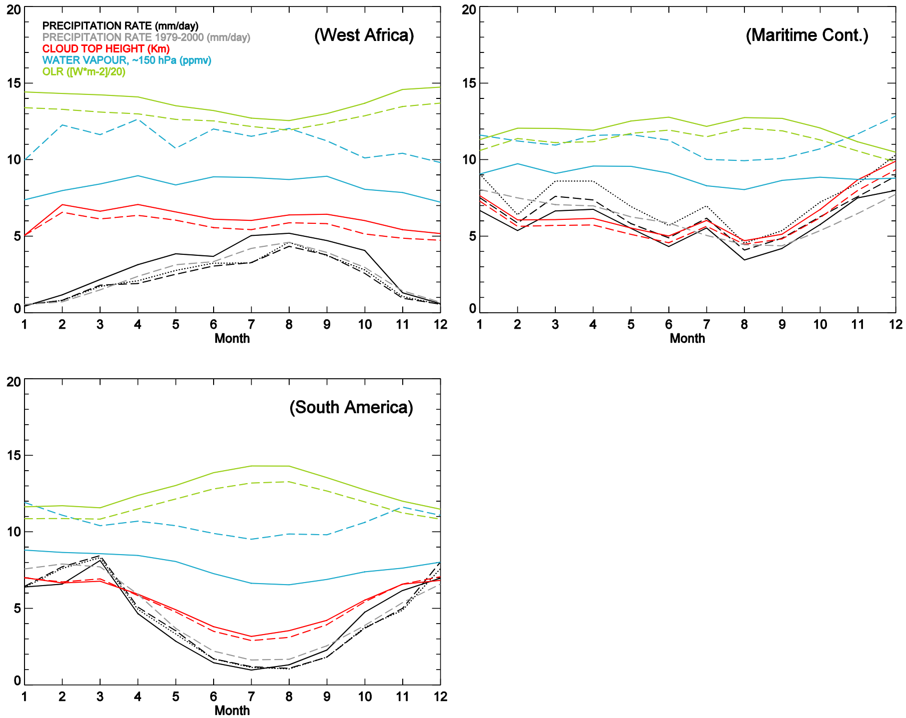

Fig. 2. Seasonal cycle of convection for 2005 averaged over West Africa, Maritime Continent, South America. Precipitation rates in black from TRMM (solid line), GPCP (dashed line), CMAP (dotted line); cloud top heights in red from MODIS-terra (solid line) and MODIS aqua (dashed line); OLR in green from AIRS (solid line) and NOOA (dashed line); water vapour in light blue from AIRS at 150 hPa (solid line) and AURA-MLS at 147 hPa (dashed line). Additionally, the grey curve shows the seasonal cycle of precipitation rates in mm/day for the GPCP long-term climatology (1979–2000).

ACPD
10, 19469–19514, 2010

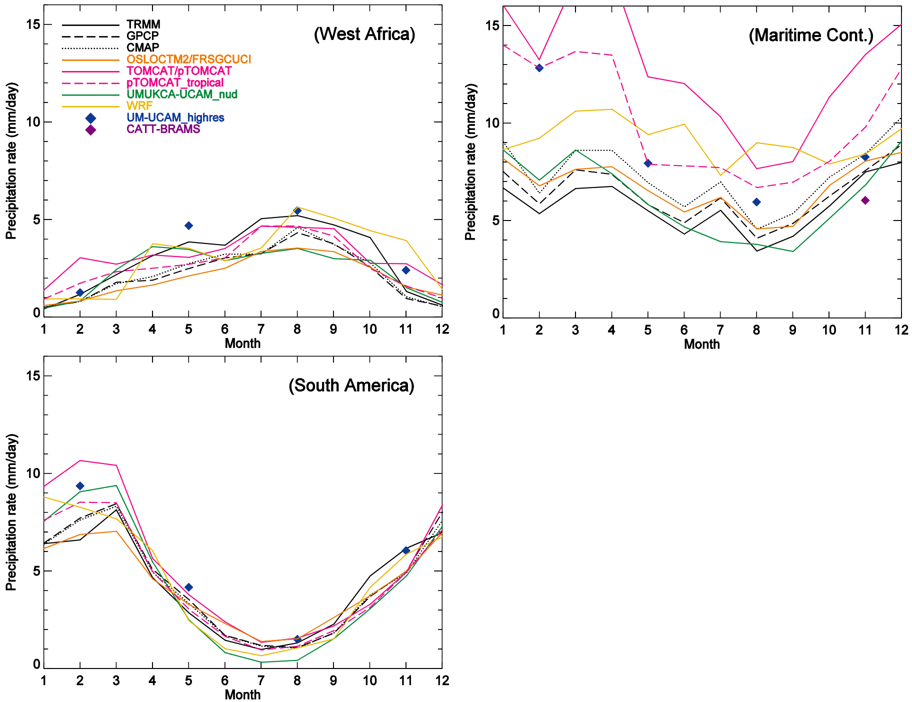

Fig. 3. Seasonal cycle of surface precipitation rate for the year 2005 from observations (TRMM, GPCP and CMAP) and model simulations, averaged over West Africa, the Maritime Continent and South America.

ACPD
10, 19469–19514, 2010

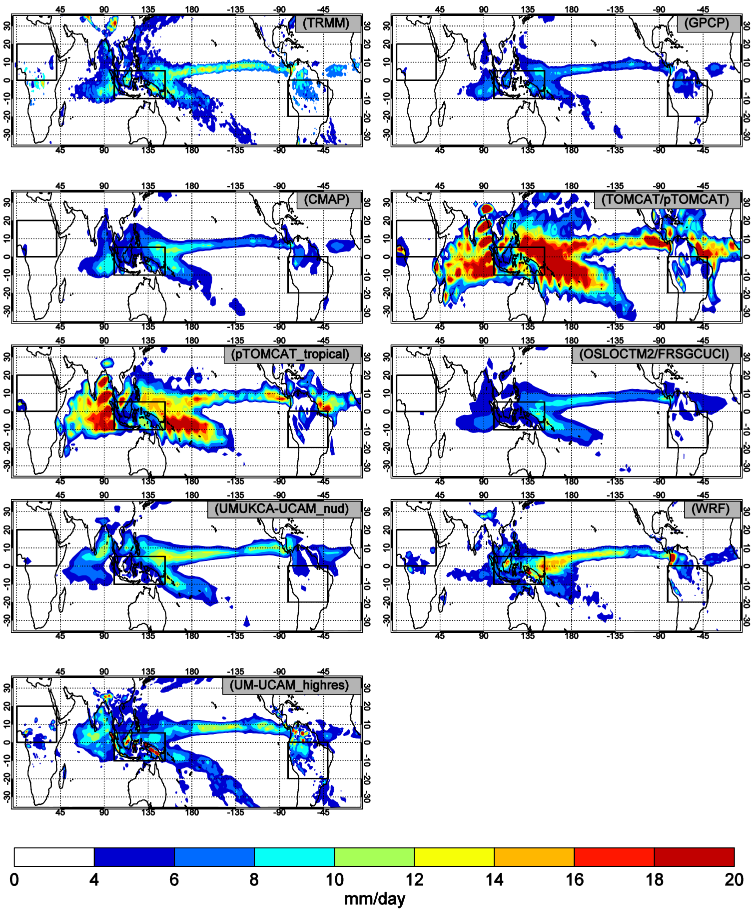

Fig. 4. Annual mean precipitation rates for the year 2005: observations (TRMM, GPCP and CMAP) and model simulations. Note that for UM-UCAM_highres the plot shows an average for the months of Febuary, May, August and November.

ACPD
10, 19469–19514, 2010

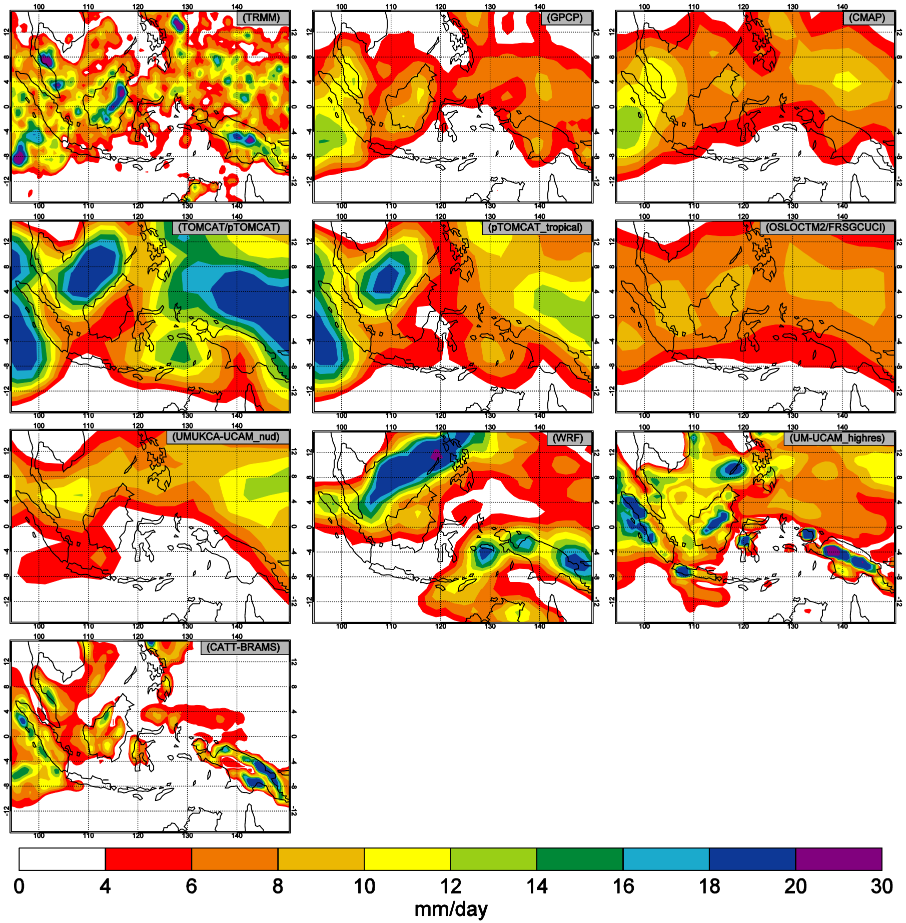

Fig. 5. Monthly mean precipitation rates in the Maritime continent for November 2005: observations (TRMM, GPCP and CMAP) and model simulations.

ACPD
10, 19469–19514, 2010

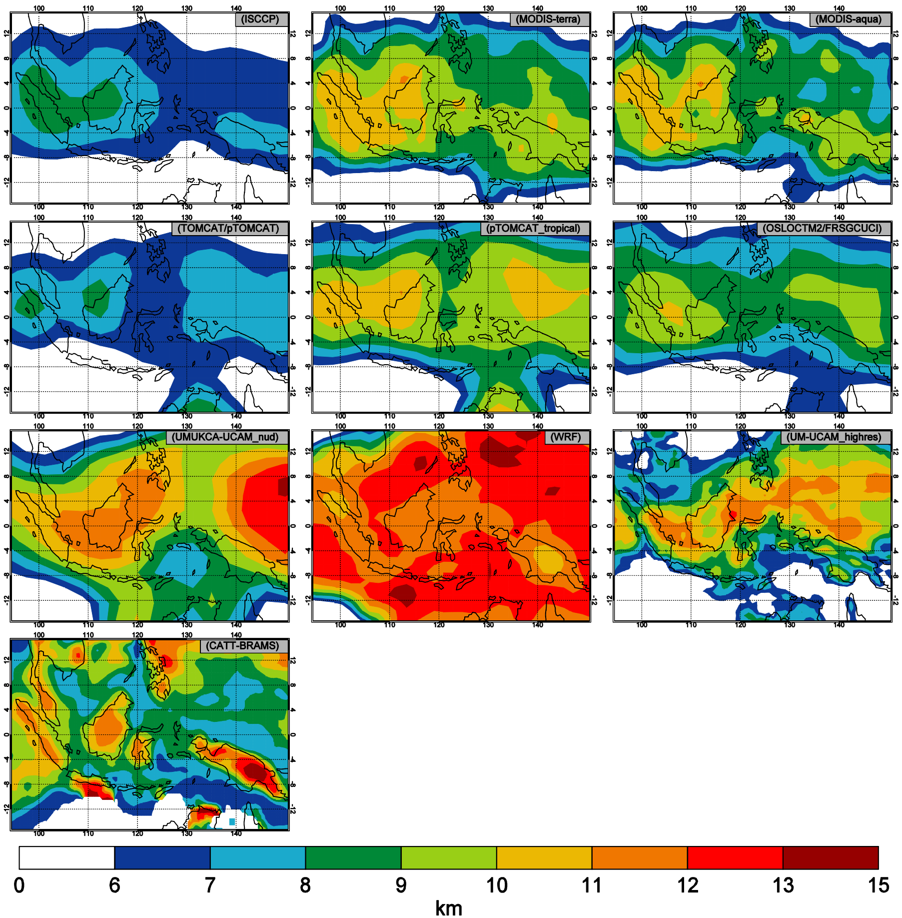

Fig. 6. Monthly mean cloud top height in the Maritime continent region for November 2005: observations (ISCCP, MODIS-terra, MODIS-aqua) and model simulations. The monthly mean values are calculated from 3-hourly data except for the two MODIS datasets, for which only daily values are available.

ACPD
10, 19469–19514, 2010

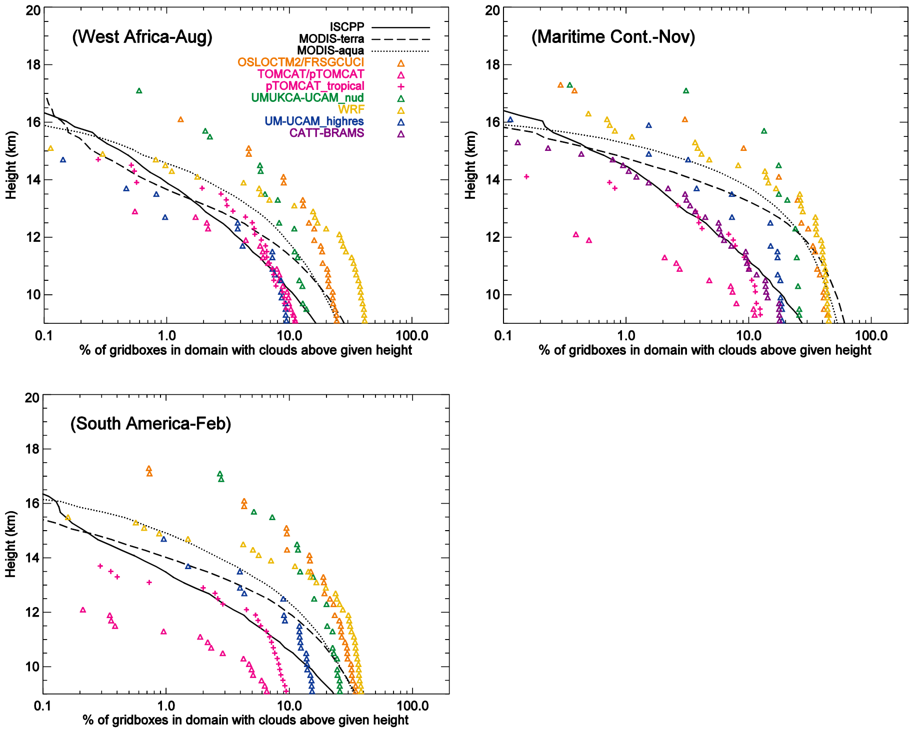

Fig. 7. Percentage of gridboxes in each domain with cloud top height above given height from observations (ISCCP, MODIS-terra, MODIS-aqua) and model simulations, calculated for West Africa in August, the Maritime Continent in November and South America in February (all months in 2005). The statistical distribution of cloud top heights within each domain is calculated from 3-hourly data, with the exception of MODIS -terra and -aqua for which only daily values are available.

ACPD
10, 19469–19514, 2010